

MICROCHEMICAL AND MICROSTRUCTURAL PROPERTIES OF METALLIC NITRIDE AND CARBIDE HARD COATINGS DEPOSITED BY ARC-EVAPORATION

M. BRAIC, V. BRAIC, M. BALACEANU,
G. PAVELESCU, A. VLADESCU

National Institute for Optoelectronics, P.O. Box MG 5, Bucharest-Magurele, Romania

(Received July 15, 2003)

Abstract: TiN, TiC, ZrN, Ti(C,N), (Ti,Zr)N and (Ti,Al)N hard coatings were deposited on Si, stainless steel and high-speed steel substrates by the cathodic arc method. The chemical composition, surface chemistry, phase composition and texture of the coatings were determined by elastic recoil detection analysis (ERDA), energy – dispersive X-ray (EDX) spectroscopy, X-ray photoelectron spectroscopy (XPS) and X-ray diffraction (XRD). The influence of the main deposition parameters (reactive gas pressure, arc current, substrate bias) on the film characteristics was investigated.

Key words: hard coatings, cathodic arc technique, ERDA, EDX, XPS, XRD.

1. INTRODUCTION

Hard coatings based on transition metal nitrides and carbides are widely used today to protect materials against wear, abrasion and corrosion [1] – [4]. Due to their remarkable properties such as high microhardness, chemical inertness, high wear and abrasion resistance, these coatings are employed in various machining applications to improve the performance of tools and mechanical components.

In this paper, synthesis and characterization of TiN, TiC, Ti(C,N), ZrN, (Ti,Zr)N and (Ti,Al)N films prepared under different deposition conditions by a cathodic arc system are presented. Various investigation techniques – elastic recoil detection analysis (ERDA), energy – dispersive X-ray (EDX) spectroscopy, X-ray photoelectron spectroscopy (XPS) and X-ray diffraction (XRD) – were used to analyze the main microchemical and microstructural characteristics of the coatings (elemental composition, surface chemistry, phase composition and texture). These properties are strongly related to functional film characteristics such as tribological performance or corrosion resistance.

2. EXPERIMENTAL DETAILS

The experimental setup has been described elsewhere [5]. Hard coatings deposition was performed on different substrates (Si, stainless steel, high-speed steel). The base pressure in the deposition chamber was of about 10^{-3} Pa. Specimens to be coated were ultrasonically cleaned with trichloroethylene and mounted on a rotating holder inside the chamber. Prior to deposition, the samples were sputtered by Ti or Zr ion bombardment (1000 V; 5 min.).

The main process parameters for the various coatings were as follows: cathode material - Ti, Zr, Al; reactive gas - N_2 , CH_4 (or C_2H_2); gas pressure $p_{gas} = 3 \times 10^{-3} \div 1$ Pa; arc current $I_a = 60 \div 120$ A; substrate bias $V_s = 15 \div 220$ V; substrate temperature $T = 160 \div 340^\circ C$; deposition time $t = 15 \div 90$ min. For the multiphase compounds deposition (Ti, Zr)N and (Ti,Al)N, different pairs of cathodes were used (Ti + Zr and Ti + Al, respectively) in a N_2 atmosphere, whereas for Ti(C,N) preparation, the reactive gas consisted of a mixture of N_2 and CH_4 (or C_2H_2).

The chemical composition of the films was determined by ERD and EDX techniques. For ERD measurements an incident 80 MeV Cu^{10+} was used. The detector of the elastically scattered recoils consisted in an ΔE pulse ionization chamber and a residual energy silicon detector placed inside the ionization chamber. Both the angle of incidence and the angle of exit were 75° relative to the sample normal. The EDX investigations were carried out by means of a XL-30-ESEM TMP scanning electron microscopic. The XPS analysis was performed on a SSX-100 spectrometer

using monochromated Al K α radiation (1486.6 eV). Spectra were acquired at room temperature, in a vacuum of about 5×10^{-7} Pa, and with a take-off angle with respect to the sample normal of 55° . The analyzed area was of about 1.4 mm^2 and the pass energy was set to 150 eV. In these conditions, the resolution, as determined by the full width at half maximum (FWHM) of the Au $4f_{7/2}$ peak of a standard gold sample, was around 1.6 eV. Phase composition and texture were obtained by XRD analysis using an X-ray DRON diffractometer with CuK α radiation.

3. RESULTS AND DISCUSSION

3.1. Elemental composition

ERD method was used for the investigation of the TiN films deposited at different N_2 pressures. A typical example of ERD spectra from a TiN film is shown in Fig. 1, where the computer simulation curve is also plotted (deposition conditions: $p_{\text{N}_2} = 10^{-2}$ Pa, $V_s = 220$ V, $I_a = 90$ A). In this case the film composition was: Ti – 44.6%, N – 53.5%, O – 1.3%, C – 0.6%, from which an N/Ti ratio of 1.2 was calculated. The presence of a small amount of oxygen and carbon is due both to residual gas incorporated in the chamber walls and to the contamination during sample handling in open atmosphere before the composition analysis.

The influence of the N_2 pressure on the N/Ti ratio is shown in Fig.2. It can be seen that the variation of the N_2 pressure in the range $10^{-2} \div 1$ Pa only slightly influences the film stoichiometry, while a decrease of the pressure in the range $10^{-2} \div 5 \times 10^{-3}$ Pa results in a diminishment of N/Ti coefficient from 1.2 to 0.7 .

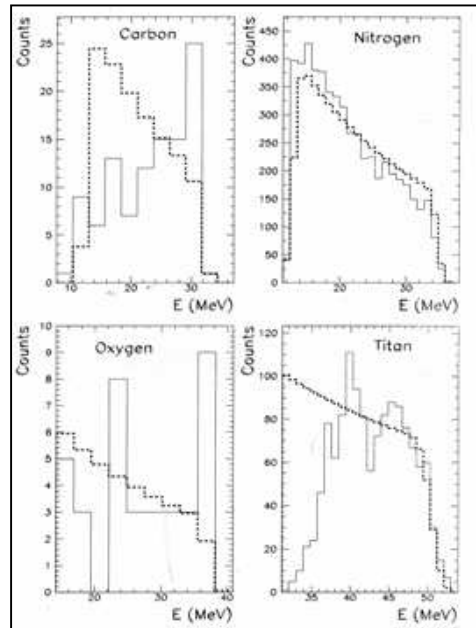


Fig.1- ERD spectra of Ti, N, O and C for a TiN coating

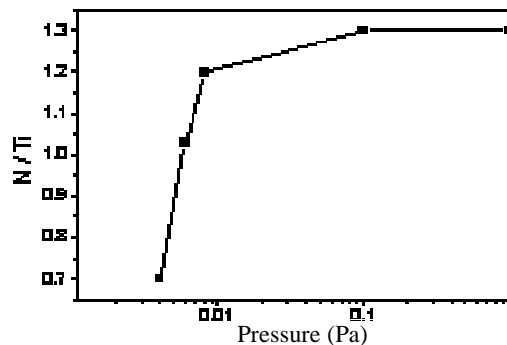


Fig. 2- N/Ti ratio as a function of N_2 pressure

In the case of the ternary compounds (Ti,Al)N, (Ti,Zr)N and Ti(C,N), the elemental composition of the coatings was obtained by EDX analysis. Examples of EDX spectra for (Ti, Al)N and (Ti,Zr)N films are given in figures 3 and 4, respectively. The deposition conditions for these films were: (Ti,Al)N – $p_{N_2} = 10^{-1}$ Pa, $I_{Al} = 50$ A, $I_{Ti} = 90$ A, $V_s = 220$ V; (Ti,Zr)N – $p_{N_2} = 10^{-1}$ Pa, $I_{Zr} = 120$ A, $I_{Ti} = 90$ A, $V_s = 220$ V, where I_{Ti} , I_{Al} and I_{Zr} are the currents at the cathodes of Ti, Al and Zr, respectively. The chemical compositions of the films are given in Table 1.

Table 1
Chemical composition of (Ti, Al)N and (Ti, Zr)N coatings

Film	Elemental concentration (at. %)					
	Ti	Al	Zr	Fe	N	O
(Ti,Al)N	30.9	14.8	-	2.0	43.6	8.7
(Ti,Zr)N	15.3	-	33.0	0.8	49.7	1.2

For these cases, the coatings were almost stoichiometric (the ratios $N/(Ti + Al)$ and $N/(Ti + Zr)$ are of 0.95 and 1.03, respectively). As it is known (e.g. [6], [7]), Ti/Zr or Ti/Al ratios have a marked influence on the film properties. Our experiments showed that the Ti/Zr or Ti/Al ratios can be controlled mainly by the arc current values at the corresponding cathodes. For example, an increase of the I_{Ti} from 50 to 90 A resulted in an enhancement of the Ti/Al ratio from 0.74 to 2.09 (I_{Al} was kept constant at 50 A). The experiments also revealed that for the Ti(C,N) coatings, the N/C ratio was almost the same (within 5-10%) as that given by the ratio of the reactive gas composition, which was controlled through the gas flow rates of N_2 and gas containing carbon (CH_4 or C_2H_2).

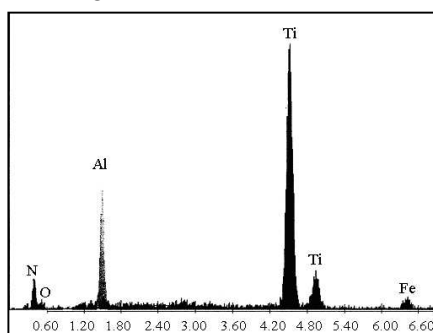


Fig. 3
EDX spectrum for a (Ti,Al)N coating

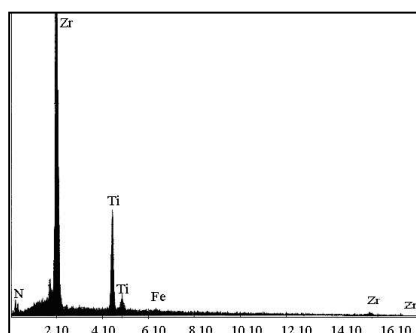


Fig. 4
EDX spectrum for a (Ti,Zr)N coating

3.2. Surface chemistry

The compounds formed on the TiN coatings surface (up to a maximum depth of 10 Å) were determined by XPS [5]. The deposition conditions for the films investigated are listed in Table 2.

Table 2
Deposition parameters for the TiN coatings

Sample	Deposition parameters			
	P_{N_2} (Pa)	V_s (V)	I_a (A)	t (min)
1	2×10^{-2}	225	60	15
2	8×10^{-2}	225	60	15
3	5×10^{-1}	225	60	15
4	8×10^{-2}	50	60	15

An example of XPS spectra (sample 1) for Ti 2p, N 1s and O 1s peaks is shown in Fig. 5, where the peak-fitting procedure, using mixed Gauss/Lorentz (85% G/L) functions, is also presented. From the spectra analysis (Table 3), it resulted that the coatings are composed from a basic TiN compound, cvasistoichiometric (N/Ti \approx 1), covered by an oxidized layer, consisting of a mixture of Ti₂O₃ and TiNO, with relative concentrations depending on the deposition parameters.

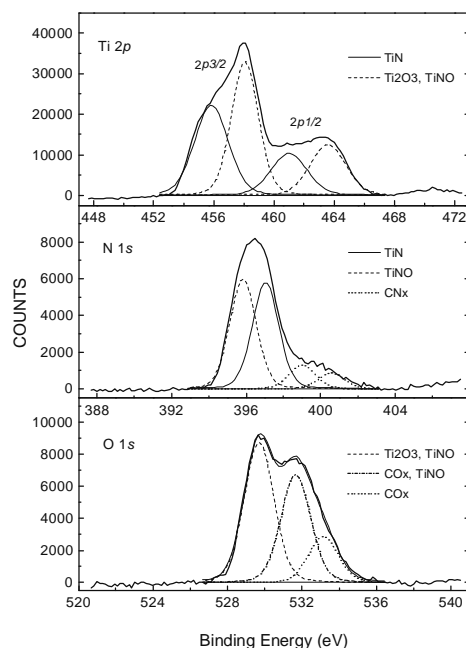


Fig.5.- XPS spectra for Ti 2p, N 1s and O 1s

Table 3

The binding energies (in eV) of the XPS peaks and the atomic concentration of the corresponding phases

Sample	C		Ti		N			O	
	C-C	C-(O, N) bonds	TiN	Ti ₂ O ₃ TiNO	TiNO	TiN	C-N bonds	Ti ₂ O ₃ TiON	C-O bonds
1	284.8 45.0%	286.2, 288.4 10.7%	455.8 4.9%	458.1 5.9%	395.8 4.5%	397.0 4.4%	399.0, 400.6 1.6%	529.7 10.9%	531.7, 533.1 12.0%
2	284.8 37.9%	286.2, 288.4 10.5%	456.1 6.4%	458.2 7.2%	396.0 6.1%	397.2 5.7%	399.1, 400.8 1.9%	529.9 12.5%	531.7, 533.3 11.8%
3	284.7 33.5%	286.2, 288.3 8.8%	455.9 6.2%	458.1 9.5%	395.9 7.0%	397.2 6.1%	399.0, 400.8 2.0%	529.9 14.6%	531.6, 533.1, 535.4 12.3%
4	284.7 37.9%	286.3, 288.4 9.2%	455.6 6.4%	458.0 8.6%	396.0 4.6%	397.1 8.6%	398.9, 400.5 2.5%	529.8 11.9%	531.7, 533.3 10.4%

3.3. Phase composition and texture

3.3.1. Binary compounds TiN, ZrN and TiC

For the binary compounds of type Ti-N, Zr-N and Ti-C, X-ray diffraction patterns revealed that the coatings consisted, in the most cases, of only the phases δ -TiN, ZrN and TiC, respectively. However, at low pressures of the reactive gas, slight diffraction peaks of the metal were also detected (e.g. Ti(110) line, Fig. 7). Typical diffraction patterns for TiN, ZrN and TiC are illustrated in figures 6 and 7, respectively. One may observe a strong (111) preferred orientation, as it was commonly reported for the films deposited by this method [8], [9]. This particular

orientation was predicted under the deposition conditions in which the strain energy was dominant as compared to the surface energy.

Under particular deposition conditions ($p_{N_2} < 10^{-2}$ Pa; $V_s < 20$ V), the TiN coatings exhibited a texture with no preferred orientation (the only detected lines, (111) and (200), had almost the same intensities).

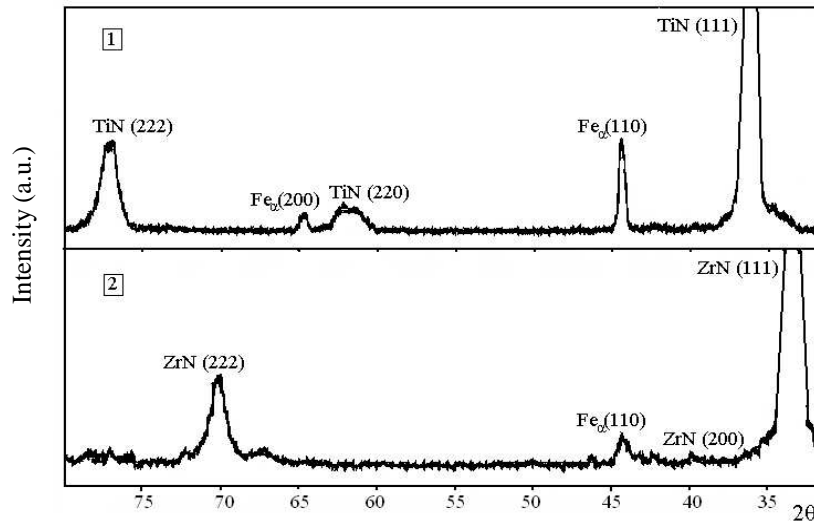


Fig. 6- X-ray diffraction patterns for TiN (1) and ZrN (2) coatings

A change of the texture with the variation of the deposition conditions was also observed for the TiC coatings (Fig.7). For certain deposition parameters (reactive gas – C_2H_2 , gas pressure – $4 \times 10^{-2} \div 6 \times 10^{-2}$ Pa, $V_s > 100$ V), a typical X-ray diffraction pattern (Fig.7(1)) exhibits slight and broad diffraction peaks, suggesting that nanocomposite coatings were formed. Following the deconvolution procedure of the line profile described in [10], crystallite size lower than 10 nm was calculated. It is worth noting that such coatings are superhard, with Vickers microhardness exceeding 4000 HV (the maximum value were of about 5200 HV [11],[12]). One may presume that these films consist of nanocrystals of TiC imbedded in an a-C:H matrix, the mechanism of the phase segregation being similar to that leading to the formation of the nc – TiN/a – Si_3N_4 nanocomposite (the most studied superhard nanocomposite) [13].

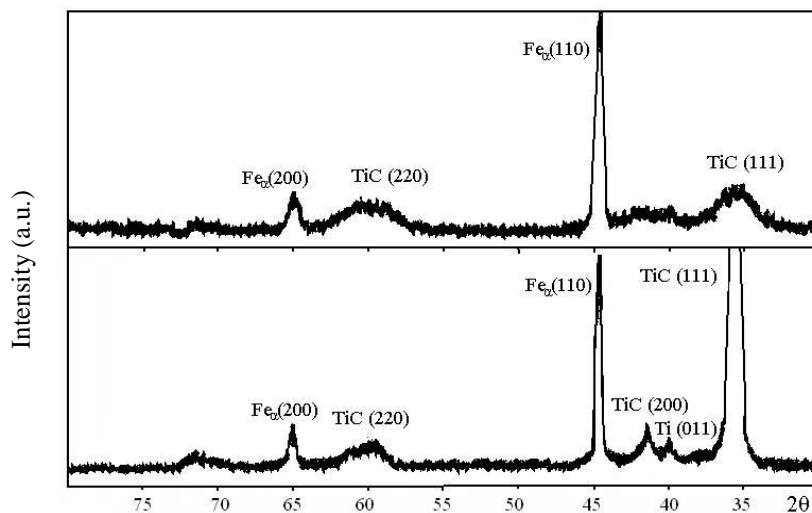


Fig.7- X-ray diffraction patterns for TiC coatings
1- with C_2H_2 ; 2- with CH_4

3.3.2. Ternary compounds (Ti,Al)N, (Ti,Zr)N and Ti(C,N)

As in the case of the binary compounds, the (Ti,Al)N and (Ti,Zr)N coatings generally exhibited a texture with a strong (111) orientation. Two X-ray diffraction patterns for (Ti,Al)N coatings with different Ti/Al ratios are shown in Fig.8. The intensity of the (111) (Ti,Al)N line

increases with the current at the Ti cathode. It can also be observed the diffraction peaks belonging to Al, indicating that some of the aluminium atoms did not react with nitrogen. Similar behavior was found for the (Ti,Zr)N coatings (Fig.9): the intensities and the position of the lines depended significantly on the currents at the Ti and Zr cathodes.

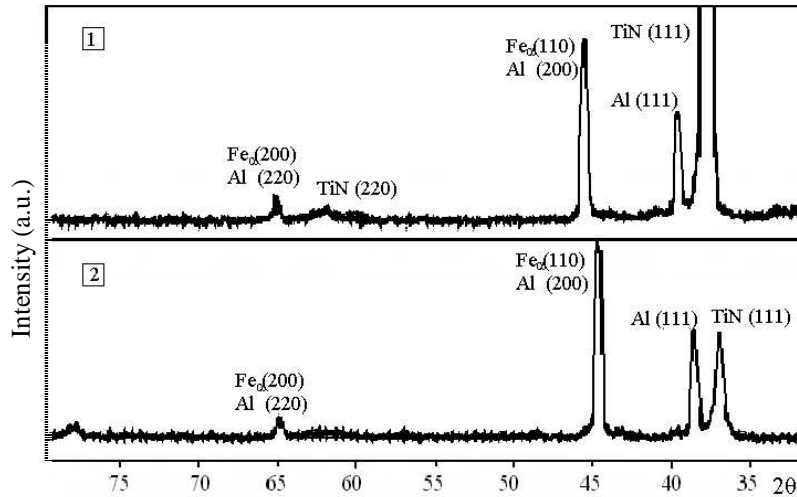
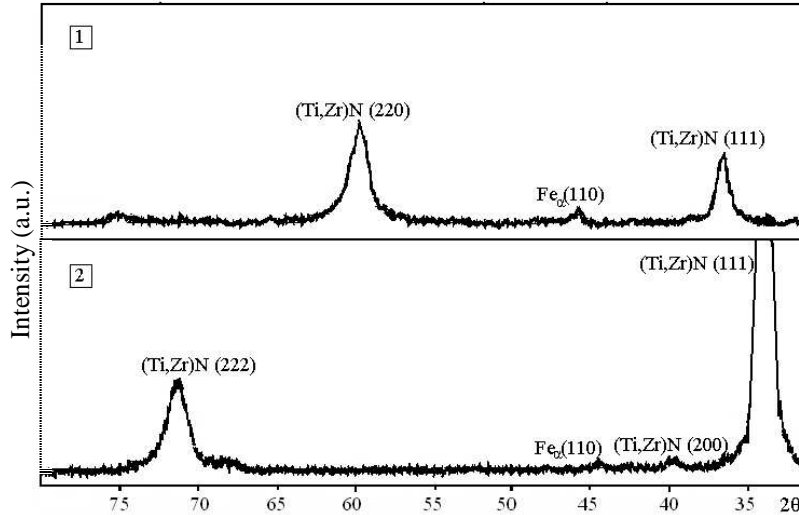


Fig.8- X-ray diffraction patterns for (Ti,Al)N
 1 - $I_{Ti} = 90$ A, $I_{Al} = 50$ A;
 2 - $I_{Ti} = 50$ A, $I_{Al} = 50$ A



For the Ti(C,N) coatings, the diffraction lines ((111), (200) and (220)) were positioned between TiC and TiN lines, according to the ASTM specifications. An increase of the nitrogen concentration results in a stronger (111) orientation and in a displacement of the lines towards higher Bragg angles. This latest effect can be accounted for by the replacement of the carbon atoms in the TiC lattice by nitrogen atoms, which have smaller dimensions.

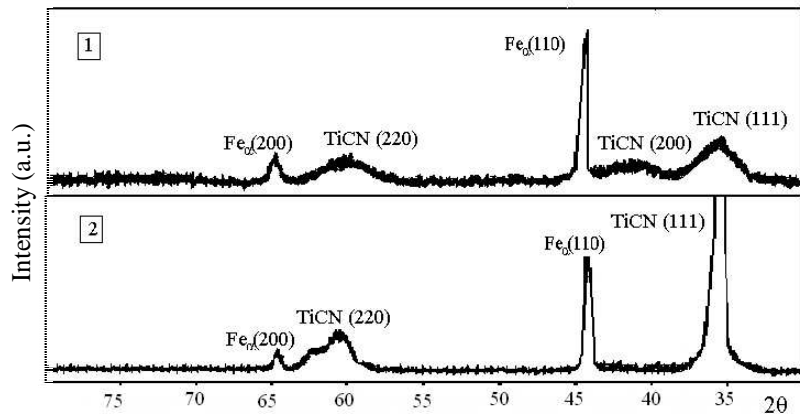


Fig.10- X-ray diffraction patterns for (TiC_{0.6}N_{0.4})

1 – with CH₄; 2 – with C₂H₂

Similar to the TiC films, significant differences were observed between the diffraction patterns of the (Ti,C)N films prepared either with CH₄ or with C₂H₂ (Fig.10). For the last case, the peaks are broader and smaller, specific to a nanostructured film. These coatings are superhard [11], with microhardness increasing from 4000 to 4600 HV for an increase of the carbon content in the film in the range 0.5 ÷ 0.8. For a carbon content lower than 0.4 ÷ 0.5, the microhardness had the values (2500 ÷ 3100 HV) currently reported in literature.

4. SUMMARY AND CONCLUSIONS

Various binary (TiN, TiC, Zr) and ternary ((Ti,Al)N, (Ti,Zr)N, Ti(C,N)) metallic hard materials were deposited on Si and steel substrates by cathodic arc technique. The influence of the main deposition parameters (reactive gas pressure, arc current, substrate bias) on the chemical composition, surface chemistry, phase composition and texture of the coatings was investigated in order to select the most suitable conditions to prepare high quality films.

ERD analysis revealed the dependence of the film stoichiometry N/Ti on the N₂ pressure for the TiN coatings. It was found that the N/Ti ratio, with a value of about 1.2, did not depend on the N₂ pressure in the range 10⁻² ÷ 5x10⁻³ Pa, whereas a variation of the pressure from 10⁻² to 5x10⁻³ Pa led to a decrease of N/Ti from 1.2 to 0.7. EDX technique was used to determine the elemental composition of the ternary compounds (Ti,Al)N, (Ti,Zr)N and Ti(C,N). The experiments showed that the Ti/Zr and Ti/Al ratios, which have a significant influence on the film properties, can be efficiently controlled by the arc currents at the corresponding cathodes. In the case of Ti(C,N) films, the gas flow rates of N₂ and gas containing carbon (CH₄ or C₂H₂) decide the N/C ratio in the coating composition.

From XPS spectra examination, the elemental composition and the chemical bindings existing at the surface of the TiN coatings were obtained. It was found that a basic cvasistoichiometric TiN compound was covered by a layer consisting of a mixture of Ti₂O₃ and TiNO.

XRD analysis revealed that, in general, the binary metallic coatings TiN, ZrN and TiC exhibited a strong (111) preferred orientation. However, under particular deposition conditions, a texture with no preferred orientation was found. In the case of TiC, the coatings with such a texture exhibited very high microhardness values, up to 5200 HV. For the ternary compounds (Ti,Al)N and (Ti,Zr)N, the intensities and positions of the diffraction peaks depended mainly on the currents at the corresponding cathodes. As for the Ti(C,N) coatings, different diffraction patterns were observed when CH₄ or C₂H₂ were used for the film preparation: a strong (111) orientation in the first case and no preferred orientation in the second one. For these last coatings, high microhardness values were measured (4200 - 4600 HV).

REFERENCES

1. *Handbook of Deposition Technologies for Films and Coatings*, ed. R.F. Bunshah, Noyes, New Jersey, 1995.
2. H. Holleck, *Designing Advanced Coatings for Wear Protection*, Surf.Eng. **7**, 137- 144, 1991.
3. D.S. Rickerby, A. Matthews, *Advanced surface Coatings – A Handbook of surface Engineering*, Blackie and Sons, London, 1991.
4. *Protective Coatings and Thin Films*, Kluwer Academic Publishers, Dordrecht/Boston/London, 1997.
5. M. Balaceanu, M. Braic, D. Macovei, M.J. Genet, A. Manea, D. Pantelica, V. Braic, F. Negoita, *Properties of titanium based hard coatings deposited by the cathodic arc method*, J. Optoelectron. Adv. Mater., **4**, 107-114, 2002.
6. Da-Young Wang, Chi-Lung Chang, Cheng-Hsun Hsu, Hua-Ni Lin, *Synthesis of (Ti,Zr)N hard coatings by unbalanced magnetron sputtering*, Surface and Coatings Technology, **130**, 64 – 68, 2000.
7. Da-Young Wang, Yen-Way Li, Chi-Lung Chang, Wei-Yu Ho, *Deposition of high quality(Ti,Al)N hard coatings by vacuum arc evaporation process*, Surface and Coatings Technology, **114**, 109-113, 1999.
8. J. Vyskočil and J. Musil, *Cathodic arc evaporation in thin film technology*, J.Vac.Sci.Technol.A., **10**, 1740 –1748, 1992.
9. D.C. Kothari, A.N. Kale, *Recent trends in surface engineering using cathodic arc technique*, Surface and Coatings Technology, **158-159**, 174-179, 2002.
10. R. Delhez, Th.H. de Keijser and E.J. Mittemeijer, *Role of X-ray diffraction analysis in surface engineering: investigation of microstructure of nitrided iron and steels*, Surface Engineering, **3**, 331-342, 1987.
11. V. Braic, M. Braic, M. Balaceanu, G. Pavelescu, *Influence of the reactive gases nature on Ti(C,N) hard coatings in cathodic vacuum arc deposition*, Proc. XXth International Symposium on Discharges and Electrical Insulation in Vacuum, Tours, France, 166-169, 2002.

12. M. Balaceanu, V. Braic, I. Tudor, M. Braic, G. Pavelescu, A. Popeacu, F. Ionescu, *Cathodic arc deposition of superhard TiC and Ti(C,N) coatings*, Proc. 3rd Intern.Conf. „*Ti*” Coatings in Manufacturing Engineering, Thessaloniki, Greece, 271-279, 2002
13. Stan Vepřek, *The search for novel, superhard materials*, J. Vac. Sci. Technol. A. **17**(5), 2401-2420, 1999.